Spectral Color Management using Interim Connection Spaces based on Spectral Decomposition

Shohei Tsutsumi[*†], Mitchell R. Rosen[†] and Roy S. Berns[†]*
[*]Canon Inc.; Tokyo, Japan;
[†]Munsell Color Science Laboratory, Rochester Institute of Technology; Rochester, New York, USA

Abstract

A feasible approach to spectral color management was previously defined to include lookups performed within an interim connection space (ICS). The ICS is situated between a high-dimensional spectral profile connection space and output units. The definition of ICS axes and the minimum number of ICS dimensions are explored through consideration of LabPQR, an ICS described in earlier work. LabPQR has three colorimetric dimensions (CIELAB) and additional dimensions to describe a metameric black (PQR). Several versions of LabPQR are explored. One type defines PQR axes based on metameric blacks generated from Cohen and Kappauf's spectral decomposition. The second type is constructed in an unconstrained way where metameric blacks are statistically derived based on the spectral characteristics of the target output device. For a six-dimensional LabPQR, one that uses three colorimetric and three metameric black dimensions, it was found that Cohen and Kappauf-based LabPQR was inferior for estimating the spectra when compared to the unconstrained method. However, when the limited spectral gamut of an output device was introduced through printer simulation and necessary spectral gamut mapping, the disadvantage of six-dimensional Cohen and Kappauf-based LabPQR dissipated. On the other hand, reducing LabPQR to only five-dimensions (two metameric black dimensions) reintroduced the advanatage of the unconstrained approach even after virtual printer was consulted and spectral gamut mapping calculated. Importantly, it was found that the five-dimensional unconstrained approach achieved equivalent levels of performance to a full 31-dimensional approach within simulated printer spectral gamut limitations.

Introduction

An important goal of spectral color management is to reproduce images that match originals under arbitrary illuminants. Spectral reproduction requires new approaches including spectral profiling of devices, spectral profile connection spaces (PCSλ), spectral image processing and new quality metrics. Spectral color management will take advantage of all these concepts and require transformation chains that deliver high-quality results quickly.

In previous research [1]-[3], a spectral reproduction workflow from scene to hardcopy was proposed. One of the difficulties associated with spectral reproduction is its high dimensionality since more information is necessary for reproducing samples with illuminant-independence than needed for more traditional colorimetric reproduction. The proposed workflow included a step where spectra of high dimensionality were converted to a lower-dimensional encoding known as an interim connection space (ICS) [3]-[4].

Derhak and Rosen proposed an ICS called LabPQR [5]-[6]. LabPQR is an ICS that has three colorimetric axes (CIELAB) plus additional spectral reconstruction axes (PQR). PQR describes a stimulus' metameric black [7]-[8], a spectral difference between the actual spectra and a spectra derived from only knowledge of the CIELAB components. In a transformation from the colorimetric encoding, a spectrum is derived from CIELAB values and is combined with a meteric black derived from the PQR encoding. One approach described in the literature for building LabPQR [5] uses the spectral gamut of a particular output device to derive the transformation from CIELAB to a metamer. This device-dependence of LabPQR as an ICS does not violate device independence assumptions of color management because the ICS is utilized on the output side of the PCSλ. The PCSλ is still device independent. All ICS information could sit within the output device profile. This information could include the transformation from spectral units to ICS.

Device-independence of ICS is not a requirement for spectral color management. However, it may be desirable to move toward a generalized ICS so that real-time spectral image processing can be standardized. Since the PQR dimensions of LabPQR describe a metameric black, generalization would include defining a metameric black that is independent of the spectral gamut of any particular output device.

Wyszecki hypothesized a fundamental spectral stimulus for every tristimulus value and a specific metameric black that would represent an object's particular spectral characteristics [7]. Cohen and Kappauf proposed spectral decomposition scheme know as "matrix-R" [9]-[10]. The matrix-R operation is based on color-matching functions weighted by a specific illuminant. It is a widely used means for composing a fundamental stimulus. For example, Cohen and Kappauf's approach is utilized for the spectral reconstruction from given colorimetric values for Fairman's parameric decomposition [11].

The spectral characterization of a printer [12] yields the forward relationship from fractional area coverage to spectra. Unfortunately, spectra are typically 31 or more dimensional values. For some spectral color management implementations, the spectra are then converted to the lower-dimensional ICS. For this discussion, we use LabPQR as the ICS. In previous research [13], an inversion of the printer characterization was successfully performed to choose fractional area coverages for a requested spectrum. In the inversion process, spectral gamut mapping [5]-[6] is necessary since an answer must be delivered for any arbitrary spectral request, even those outside of a printer's spectral gamut. A previous spectral gamut mapping proposal for LabPQR was based on a single stage optimization for minimizing both colorimetric and spectral error simultaneously [13].

In this research, LabPQR configurations are evaluated in terms of how to devise metameric black and what number of dimensions to include. Interactions between generalization and dimensions are discussed. First, constraining LabPQR, to use Cohen and Kappauf's spectral decomposition (CK-based LabPQR) is explored. The alternative spectral decomposition approach is to derive metameric black after a statistical analysis of a specific device's metamer space (unconstrained LabPQR). For several types of datasets, the spectral reconstruction accuracies for CK-based LabPQR will be illustrated and compared to unconstrained LabPQR. Quality tradeoffs between the two approaches and the number of spectral reconstruction dimensions will be examined.

Spectral Decomposition for ICS Definition

LabPQR [5] is an interim connection space (ICS) for use in spectral color management. The first three dimensions are CIELAB values under a particular viewing condition, and the additional dimensions are spectral reconstruction dimensions describing a metameric black (PQR). A six-dimensional example of LabPQR has been discussed in the literature [5]-[6] and it has been demonstrated for use in spectral gamut mapping [6], [13].

Spectral reconstruction from a six-dimensional LabPQR is as follows:

$$\hat{\mathbf{R}} = \mathbf{T}\mathbf{N}_c + \mathbf{V}\mathbf{N}_p \quad , \tag{1}$$

where $\mathbf{T}$ is a n by 3 transformation matrix where n counts wavelength, $\mathbf{V}$ is a n by 3 matrix describing PQR bases, $\mathbf{N}_c$ is a 3 by 1 tristimulus vector, and $\mathbf{N}_p$ is a 3 by 1 vector of PQR values. Here, the subscriptions for "c" and "p" imply colorimetric and PQR values, respectively. Note that $\mathbf{T}$ is applied to tristimulus values converted from CIELAB values.

Derivation of the $\mathbf{V}$ matrix depends on both the nature of the metamer created through the $\mathbf{T}$ matrix from LabPQR's CIELAB dimensions and the spectral gamut that is being described by the ICS. An approach that puts no *a priori* constraints on derivation of the $\mathbf{T}$ matrix derives it directly from the spectral space of the device being profiled. We call this $\mathbf{T}_u$ for *unconstrained*. A second LabPQR derivation is based on Cohen and Kappauf's metameric black, where no specific device is referred to in the derivation of $\mathbf{T}$. Instead, based on Cohen and Kappauf's work, $\mathbf{T}$ is determined by a n by 3 matrix of ASTM weights, $\mathbf{A}$, applicable to a specific illuminant and observer pair. This is referred to as $\mathbf{T}_{ck}$:

$$\mathbf{T}_{ck} = \mathbf{A}\left(\mathbf{A}^{\mathrm{T}}\mathbf{A}\right)^{-1} \quad . \tag{2}$$

$\mathbf{T}_{ck}$ is derived referring to Cohen and Kappauf's spectral decomposition, the so-called "matrix-R" [9]-[10]. Since the $\mathbf{T}_{ck}$ is based on the color-matching functions weighted by the defined illuminant and observer pair, the degree of device-dependency is decreased in such a LabPQR.

For both the CK-based and unconstrained LabPQR spaces tested here, PQR bases $\mathbf{V}$ are derived from Principal Component Analysis (PCA) [14] on a set of the metameric blacks specific to the device. Thus, for the unconstrained version of LabPQR, both terms on the right hand side of Eq. (1) depend on the device whereas for the CK-based approach, $\mathbf{T}_{ck}$ is constrained to be Cohen and Kappauf's matrix-R leaving $\mathbf{V}$ as the only device dependent term on the right hand side of Eq. (1).

The metameric blacks are spectral differences between the original spectra $\mathbf{R}$ and the fundamental stimuli derived from the tristimulus values, expressed as:

$$\mathbf{B} = \mathbf{R} - \mathbf{T}\mathbf{N}_c \quad , \tag{3}$$

where $\mathbf{T}$ may either be $\mathbf{T}_u$ or $\mathbf{T}_{ck}$, depending upon which approach is being used.

To make LabPQR into an ICS, only a limited number of eigenvectors should be preserved to reduce dimensions. Often the first three eigenvectors are preserved as the PQR bases:

$$\mathbf{V}_{PQR} = (\mathbf{v}_1, \mathbf{v}_2, \mathbf{v}_3) \quad , \tag{4}$$

where $\mathbf{v}_i$ are eigenvectors approximating the merameric black set.

To explore the influence of dimensional reduction in LabPQR, the spectral representation portion in Eq. (4) will be changed by reducing the numbers of dimensions, such as PQ bases and only a P basis, respectively expressed as:

$$\mathbf{V}_{PQ} = (\mathbf{v}_1, \mathbf{v}_2) \tag{6}$$

and

$$\mathbf{V}_{P} = \mathbf{v}_1 \quad . \tag{7}$$

For Eq. (6), only the first two eigenvectors are preserved making for a five-dimensional LabPQR and for Eq. (7), only the most significant eigenvector is preserved making for a four-dimensional LabPQR.

Spectral Gamut Mapping

Spectral gamut mapping can be considered from two veiwpoints: colorimetric and spectral [5]-[6]. In a previous research [13], the two were combined and considered simultaneously. Fractional area coverages of an inkjet printer for arbitrary requested spectra were computed by minimizing a single objective function: the weighted sum of CIEDE2000 color difference [15] and the normalized Euclidian distance in PQR:

$$\mathrm{ObjFunc1} = \mathrm{Minimize}(\mathrm{C\,IEDE2000} + k\Delta PQR) \quad , \tag{8}$$

where k is a weighting that may be empirically fitted.

The first term on the right hand side of Eq. (8) implies the absolute colorimetric matching based on the CIEDE2000 color difference while the second term represents spectral matching to minimize the spectral error between requested and response stimuli. Equation (8) can be globally utilized regardless of whether the requested stimuli are within the colorimetric or spectral response gamuts and is equivalent to minimizing spectral RMS error if the requested stimuli are within the colorimetric response gamut, because the Euclidian distance in PQR between a metameric pair is proportional to spectral RMS error [13]. It was found that k of 50 performed well [13].

Experimental

A Canon i9900 dye-based inkjet printer with a customized control driver was spectrally characterized for printer simulation. This printer had the capability of an eight-ink set, but only six were utilized: cyan (C), magenta (M), yellow (Y), black (K), red (R), and green (G). All samples were printed on Canon Photo Paper Pro (PR-101) photo quality inkjet glossy paper. Spectral reflectance factor in the range between 400 and 700 nm were

measured and colorimetric values were calculated under illuminant D50 and for the CIE 1931 2° standard observer.

Spectral reproduction for the CK-based and the unconstrained LabPQRs were evaluated and compared. This included round-trip transformation error independent of printer gamut limitations. In the round-trip evaluation, input spectral reflectances were converted to LabPQR and back to spectra, as illustrated in Fig. 1 (a). Spectral reproduction quality was also evaluated with printer gamut limitations taken into account. Figure 1 (b) describes the steps for evaluating the spectral reproduction accuracies. This workflow comprised the transformation from spectra to LabPQR, spectral gamut mapping to find an appropriate set of fractional area coverages for the printer simulation and derivation through the spectral printer model of the spectral reflectances that would have been printed from those area coverages. To investigate dimensionality, the round-trip computational accuracies and the reproduction accuracies at several different numbers of dimensions were measured. For convenience, the five dimensional space will be referred to as LabPQ and the four dimensional space will be referred to as LabP.

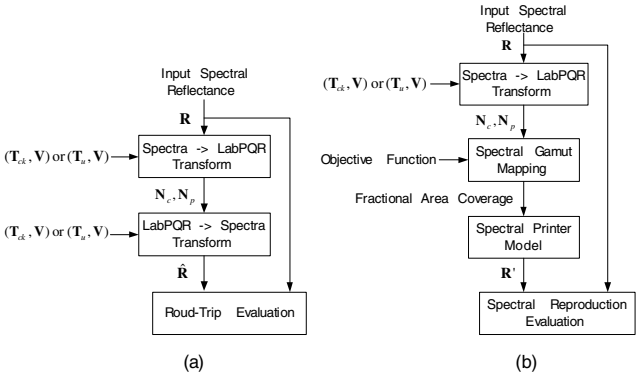

***Figure 1**. Schematic diagrams for evaluating round-trip accuracies (a) and spectral reproduction accuracies (b).*

Datasets

For the round-trip and the reproduction evaluations, a wide range of datasets were prepared:

1. A set of 729 print patches using the CMYKRG inkjet printer, which were randomly distributed in the CIELAB color space (this set is referred to as Prints)
2. GretagMacbeth ColorChecker (CC)
3. GretagMacbeth ColorChecker DC (CCDC)
4. Munsell Book of Color glossy edition containing 1600 patches (Munsell) [16]
5. A set of 120 DuPont paint chips by Vrhel *et al.* (DuPont) [17]-[18]
6. A set of 170 object spectra including plants, human skin and hair by Vrhel *et al.* (Object) [17]-[18]

Results and Discussion

Building Cohen and Kappauf-based LabPQR Transforms

CK-based LabPQR transforms consisting of the reconstruction matrices $\mathbf{T}_{ck}$ and $\mathbf{V}$ were built for each dataset. As discussed above, $\mathbf{T}_{ck}$ is derived referring to Cohen and Kappauf's spectral decomposition, expressed in Eq. (2). Coefficients of $\mathbf{T}_{ck}$ are plotted in Fig. 2 as a spectral graph.

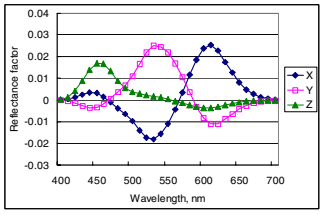

***Figure 2**. Coefficients of the reconstruction matrix $\mathbf{T}_{ck}$ for the CK-based LabPQR transform.*

Coefficients of the $\mathbf{V}$ matrix comprised of PQR bases for the Prints and the Munsell datasets were derived and plotted in Fig. 3. Although these datasets contained different types of sample populations, the curve shapes of the PQR bases were similar to one another. This could indicate device independence of LabPQR.

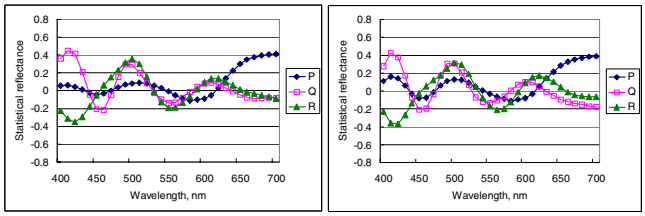

***Figure 3**. Coefficients of the **V** matrix or PQR bases of the CK-based LabPQRs for the Prints (left) and the Munsell (right) datasets.*

Building Unconstrained LabPQR Transforms

The previously defined unconstrained LabPQR method was used to define completely device-customized LabPQR transforms. Coefficients of $\mathbf{T}_u$ for the Prints and the Munsell datasets are plotted in Fig. 4. Overall, the curve shapes were similar to one another except at longer wavelengths. Since $\mathbf{T}_u$ was determined using least square analysis on a particular dataset, the coefficients were dataset dependent.

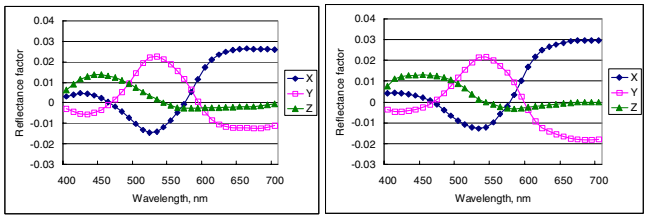

***Figure 4.** Coefficients of the reconstruction matrices $\mathbf{T}_u$ for the unconstrained LabPQR transforms for the Prints (left) and the Munsell (right) datasets.*

The coefficients of the $\mathbf{V}$ matrix or PQR bases for the Prints and the Munsell datasets are plotted in Fig. 5. As expected, each curve shapes between the datasets did not match one another. Even for the P bases, the most significant eigenvectors, the curve shapes were somewhat different from one another, and large differences were obtained in the Q and R bases. Note that the P basis for the Munsell dataset is similar to those for the CK-based LabPQRs, shown above in Fig. 3.

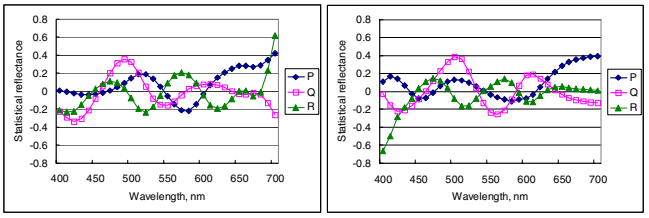

***Figure 5**. Coefficients of the **V** matrix or PQR bases of the unconstrained LabPQRs of the Prints (left) and the Munsell (right) datasets.*

Round-Trip Accuracies

Using the CK-based and the unconstrained LabPQR transforms of each dataset, the round-trip accuracies for each dataset were evaluated in terms of average spectral RMS error, summarized in Figs. 6 and 7. In the round-trip evaluation, input spectral reflectances were converted to LabPQR and back to spectra without reference to the spectral gamut of an output device. Figure 1 (a) illustrates the evaluation method. Error bars indicate 90th percentile of the spectral RMS errors. In the figures, "All" represents the LabPQR trained from a merger of all the datasets. Since the transform from colorimetric coordinates of the CK-based approaches were independent of the training datasets, their overall accuracies were worse than the unconstrained approaches.

As expected, in the unconstrained LabPQRs shown in Fig. 7, the best reconstruction was obtained when the training dataset was chosen for reconstructing its own LabPQR. That is, the LabPQR transform derived from the Prints was the most effective for verification of the Prints. It is interesting to note that in violation of intuition, for the CK-based LabPQRs shown in Fig. 6, some LabPQRs independent of the training dataset indicated better round-trip accuracies. For example, the LabPQR trained from the Munsell dataset was the best color space for the spectral reconstruction of the CC and the CCDC.

For non-training set verification, CK-based approaches were able to provide smaller difference between the different LabPQRs. When the CCDC was a verification dataset, average spectral RMS errors for the LabPQRs trained from the Prints and the CCDC were 1.34 % and 1.29 %, respectively, while they were 1.56 % and 0.92 % for the same combinations in the unconstrained LabPQRs. That is, the CK-based approach is superior for reconstructing spectra of unknown samples. In order to improve the performance of the unconstrained LabPQR, it is necessary to train it on a wide range of datasets, such as "All".

Dimensionality of the Round-Trip

Using the Munsell dataset as the verification, the round-trip accuracies at different numbers of dimensions were evaluated and are plotted in Fig. 8. In this evaluation, the CK-based and unconstrained LabPQRs built from the Prints and the Munsell datasets were utilized. The round-trip accuracies monotonically improved with increasing the number of dimensions. In particular, improvement from the four- to the five-dimensional color space, LabP to LabPQ, was large whereas the improvement from the five- to the six-dimensional color space, LabPQ to LabPQR, was relatively small. Similar trends were seen for the same analysis using LabPQR spaces derived for the Prints database. In conclusion, the CK-based approach becomes less effective in a four dimensional space but there seems to be little advantage to a six-dimensional space over a five-dimensional one.

The discussion above is important when considering the size of lookup tables (LUTs). Perhaps, the results might point the way toward abandoning the CK-based approach in order to generate smaller size of LUTs. The unconstrained approach might be appropriate in a lower-dimensional ICS such as a four-dimensional LabP.

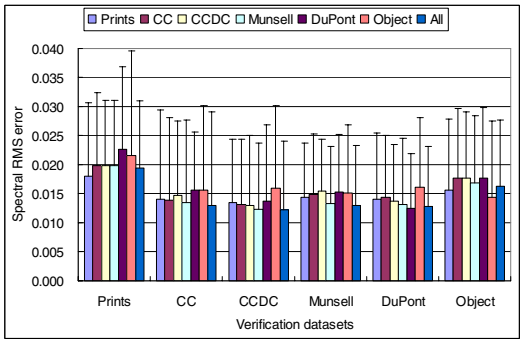

***Figure 6**. Round-trip accuracies of interaction between each dataset and each CK-based LabPQR in terms of average spectral RMS error. Error bars indicate 90th percentile of the spectral RMS errors.*

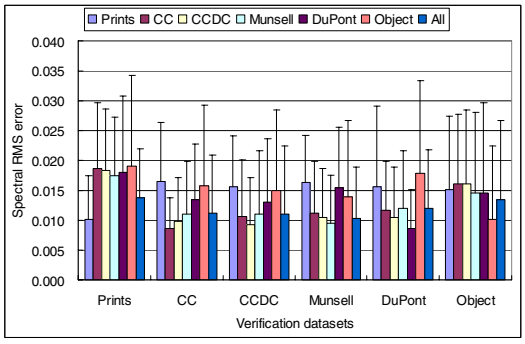

***Figure 7**. Round-trip accuracies of the interaction between each dataset and each unconstrained LabPQR in terms of average spectral RMS error.*

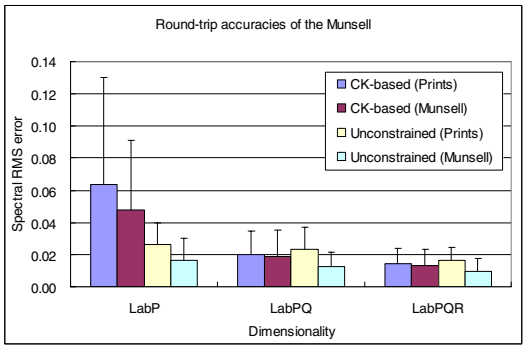

***Figure 8**. Round-trip accuracies of the Munsell dataset with the CK-based and unconstrained LabPQRs trained from either the Prints or the Munsell dataset at different dimensional LabPQRs.*

Spectral Reproduction Accuracies

In the evaluation of the round-trip accuracies, it was assumed that all requested LabPQR values were reproducible. However, it is common that the response gamut for an output device does not cover all arbitrarily requested LabPQR values, so spectral gamut mapping is necessary to choose the appropriate fractional area coverage, using the objective function [Eq. (8)].

Shown in Fig. 9 are the spectral reproduction accuracies for each dataset, with respect to average spectral RMS errors. In this evaluation, three different datasets were used for building the CK-based and the unconstrained LabPQRs: the Prints, "Identical", and "All". In case of "Identical", each LabPQR was built using the training dataset as its verification dataset. "All" is a merger of all the six datasets, as defined above. Surprisingly, for all the verification datasets, there was no significant difference between the CK-based and unconstrained LabPQRs although there had been disagreement between them in the round-trip evaluations. Similarly, there was no significant difference between results when comparing the datasets used for training. These results may reveal that a single CK-based LabPQR could be universally acceptable within the spectral color management for a six-dimensional LabPQR. Consequently, there may be no necessity to customize each LabPQR transform to each output device, if it were the case that a six dimensional ICS is acceptable.

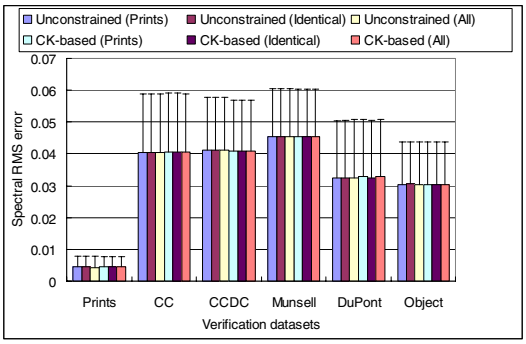

***Figure 9**. Average spectral RMS errors of each dataset in LabPQR. Three different datasets were used for building LabPQRs: the Prints, the identical dataset to the verification, and a merger of all the six datasets.*

Another interesting thing is that the reproduction accuracies for the Prints were superior to their reconstruction accuracies within the round-trip. The reproduction process including the spectral gamut mapping could cancel a lack of the spectral estimation accuracy caused by a spectra-to-LabPQR transform because the spectra synthesized by the spectral printer model were more similar to the original

Dimensionality of the Spectral Reproduction

The spectral reproduction accuracies at the different numbers of dimensions were evaluated. In addition to the dimensionality discussed above, a full 31-dimensional (Reflectance) approach and a colorimetric-only mapping (Lab) approach were examined. The Reflectance and the Lab approaches are included to show the best accuracies in terms of spectral and colorimetric-only matching, respectively.

For the Reflectance approach, instead of minimizing Eq. (8), which is based on minimizing a weighted PQR difference, an alternative objective function [Eq. (9)] minimizes a weighted spectral RMS difference:

$$\text{ObjFunc}\,2 = \text{minimize}\,(\text{CIEDE2000} + k\ \text{sRMS}), \quad (9)$$

where sRMS is the spectral RMS error. For the Lab approach, Eq. (8) was minimized where k was set to zero.

The resultant accuracies for the Munsell dataset are summarized in Figs. 10 and 11. The predicted spectra were paramerically corrected [11] such that a perfect match was obtained under illuminant D50. A CIEDE2000 color difference was calculated for illuminant A and used as a metameric index (MI) [8], shown in Fig. 11.

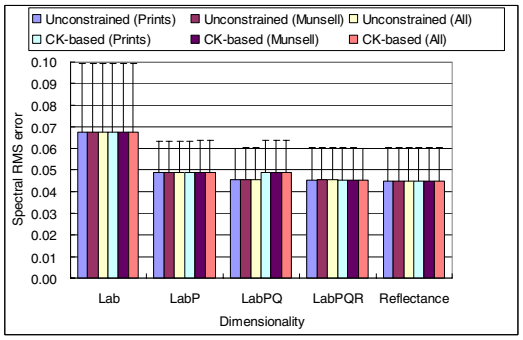

***Figure 10**. Average spectral RMS errors for the Munsell dataset at different dimensional ICSs. Three different datasets were used for building LabPQRs: the Prints, the Munsell, and a merger of all the six datasets.*

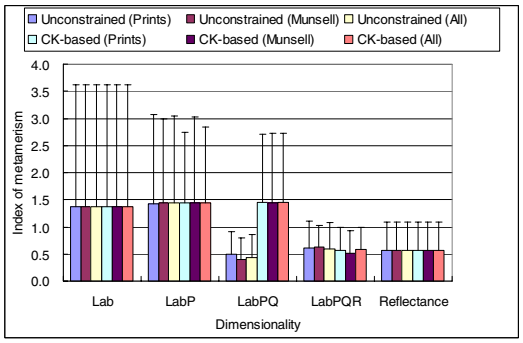

***Figure 11**. Average MIs under illuminant A for the Munsell dataset at different dimensional ICSs.*

Interestingly, the spectral differences between LabP and LabPQR become smaller than those of the round-trip in Fig. 8. This indicates that it is not necessary to use a higher dimensional ICS. Because the CMYKRG printer is not capable of reproducing any arbitrary spectral request perfectly, the ICS may have some level of spectral imprecision that can be masked by output device spectral gamut limitations. The unconstrained approaches in LabPQ were superior to the CK-based LabPQ ones while unconstrained and CK-based were equivalent in LabP and LabPQR. Similar resultant data were obtained for the other datasets.

This was a reproduction exercise with a limited spectral output gamut. Thus, even the reflectance approach had to manage error. The Reflectance approach did show the lowest spectral RMS, but their MIs were not better than those found in LabPQR or

unconstrained LabPQ. Minimizing spectral difference leads to smaller RMS, but does not guarantee achievement of the best MI for arbitrary illuminants [6]. Overall, a five-dimensional unconstrained approach was best when considering dimensionality reduction for ICS.

The sample pairs with the worst spectral RMS error (10.61 %) and the worst MI (3.17) in LabPQ are shown in Fig. 12. The spectral reconstruction at longer wavelengths, where the illuminant metamerism from illuminant D50 to A was sensitive, was poor and the reflectance factor of the reproduction was higher than that of the measured samples.

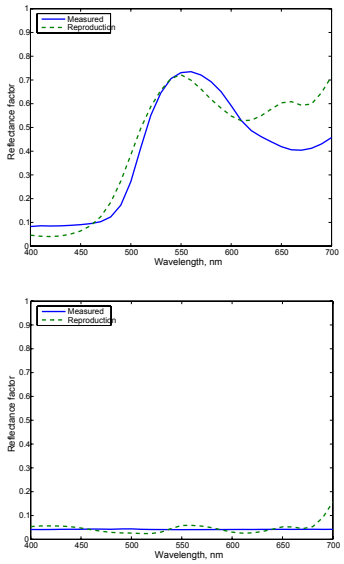

***Figure 12**. Comparisons of measured and reproduced spectra with the worst spectral RMS error (upper) and the worst MI (lower).*

Conclusions

Interim connection spaces based spectral decomposition have been explored. Variations of LabPQR were evaluated with respect to how the transformation to spectra is derived as well as the number of dimensions necessary for spectral color management. Using Cohen and Kappauf's spectral decomposition within the LabPQR definition was compared with the unconstrained approach described by Derhak and Rosen. For several datasets, after the introduction of spectral gamut mapping, the Cohen and Kappauf-based LabPQR was shown to perform as well as unconstrained LabPQR. On the other hand, for LabPQR of lower dimensions, the unconstrained approach to building LabPQR transforms showed itself superior. Also, it was found that the five-dimensional unconstrained approach was sufficient to achieve the equivalent levels of the performance to a full 31-dimensional approach for an output device with a limited spectral gamut.

A future direction of this study will be to produce a lookup-table (LUT) based on LabPQR to test actual reproduction accuracies. When attempting to produce the LUT, fewer input dimensions is obviously desirable for reducing memory size and computational cost of interpolation. Exploring the tradeoff between the LUT size and the reproduction accuracies will continue to be an important spectral color management issue.

References

[1] M.R. Rosen, F.H. Imai, X. Jiang and N. Ohta, "Spectral Reproduction from Scene to Hardcopy II: Image Processing", Proc. SPIE, **4300**, pp.33-41 (2001).

[2] M.R. Rosen, L.A. Taplin, F.H. Imai, R.S. Berns, and N. Ohta, "Answering Hunt's Web Shopping Challenge: Spectral Color Management for a Virtual Swatch", Proc. Ninth CIC, pp.267-273 (2001).

[3] M.R. Rosen, "Navigating the Roadblocks to Spectral Color Reproduction: Data-Efficient Multi-Channel Imaging and Spectral Color Management", Ph.D. Dissertation, Rochester Institute of Technology, Rochester, New York (2003).

[4] M.R. Rosen and N. Ohta, "Spectral Color Processing Using an Interim Connection Space", Proc. 11th CIC, pp. 187-192 (2003).

[5] M.W. Derhak and M.R. Rosen, "Spectral Colorimetry using LabPQR - An Interim Connection Space", J. Imaging Sci. and Technol., **50**, pp.53-63 (2006).

[6] M.R. Rosen and M.W. Derhak, "Spectral Gamuts and Spectral Gamut Mapping", Proc. SPIE, **6062**, (2006).

[7] G. Wyszecki and W. Stiles, Color Science, 2nd Edition, John Wiley & Sons (1982).

[8] R.S. Berns, Billmeyer and Saltzman's Principles of Color Technology, 3rd Edition, John Wiley & Sons (2000).

[9] J.B. Cohen and W.E. Kappauf, "Metameric Color Stimuli, Fundamental Metamers, and Wyszecki's Metameric Blacks", Am. J. Psychol., **95**, pp.537-564 (1982).

[10] J.B. Cohen, "Color and Color Mixture: Scalar and Vector Fundamentals", Color Res. Appl. **13**, pp.5-39 (1988).

[11] H.S. Fairman, "Metameric Correction Using Parameric Decomposition", Color Res. Appl. **12**, pp.261-265 (1987).

[12] Y. Chen, R.S. Berns and L.A. Taplin, "Six Color Printer Characterization Using an Optimized Cellular Yule-Nielsen Spectral Neugebauer Model", J. Imaging Sci. and Technol., **48**, pp.519-528 (2004).

[13] S. Tsutsumi, M.R. Rosen and R.S. Berns, "Spectral Reproduction Using LabPQR: Inverting the Fractional-Area-Coverage-to-Spectra Relationship", Proc. ICIS'06, pp.107-110 (2006).

[14] R.A. Johnson and D.W. Wichern, Applied Multivariate Statistical Analysis, 5th Edition, Prentice Hall (2002).

[15] M.R. Luo, G. Cui and B. Rigg, "The Development of the CIE 2000 Colour-Difference Formula: CIEDE2000", Color Res. Appl. **26**, pp.340-350 (2001).

[16] ~cs.joensuu.fi/~spectral/databases

[17] M.J. Vrhel, R. Gershon and L.S. Iwan, "Measurement and Analysis of Object Reflectance Spectra", Color Res. Appl. 19, pp.4-9 (1994).

[18] FTP from ftp.eos.ncsu.edu /pub/spectra

Author Biography

Shohei Tsutsumi received his B.E. and M.E. degrees in Electrical Engineering from Keio University, Japan in 1996 and 1998, respectively. He joined Canon Inc. in 1998 to work on development of novel approaches to image processing including halftoning and image quality. He has developed some pictorial inkjet printers such as PIXMA iP 8500 and i9900. Since 2004, he has been a visiting scientist at Munsell Color Science Laboratory, Rochester Institute of Technology. He is a member of Society for Imaging Science and Technology.